MAPPING OF 1-MHz, 45° LONGITUDINAL-WAVE FIELDS IN CENTRIFUGALLY CAST STAINLESS STEEL

M. S. Good and E. R. Green

Pacific Northwest Laboratory
Operated by Battelle Memorial Institute
Battelle Boulevard
Richland, WA 99352

INTRODUCTION

The distortion incurred by an ultrasonic field when propagating through coarse-microstructured materials was of interest. To perform an effective and reliable ultrasonic inspection, the ultrasonic field should be both spatially coherent (i.e., the field is not partitioned into multiple wave fronts traveling to different locations) and stable (i.e., field parameters such as effective refracted angle and field position do not vary sufficiently to make an inspection unreliable). Previous work indicated that the sound field emitted by a 1-MHz, 45°, longitudinal-wave probe with a 38-mm diameter transducer maintained spatial coherency while propagating through the pure microstructural forms of centrifugally cast stainless steel (CCSS) [1,2]. This analysis was extended to the mixed microstructural modes of CCSS. Furthermore, the variation of field distortion incurred by propagating through a selected microstructure was investigated by acquiring field maps from different material volumes of the same microstructural classification. To accurately map the ultrasonic field, an improved technique was used so that receiver directivity maintained a ± 1 dB sensitivity over a broad angular range centered about 45°. This report discusses the samples used, the process of mapping ultrasonic fields utilizing a 45° facet, and an analysis of multiple field maps acquired from selected CCSS microstructures.

CENTRIFUGALLY CAST STAINLESS STEEL

CCSS pipe is employed in the main coolant loop of some pressurized water reactors. This material contains a coarse microstructure that is an anisotropic-nonhomogeneous propagating material. The major microstructural classifications are a columnar, an equiaxed, and a mixed columnar-equiaxed microstructure of which the majority of field material is believed to be the latter. (See Good and Van Fleet for macrographs of each microstructure [1].)

Four CCSS materials were used to acquire ultrasonic field maps: an equiaxed microstructure, a columnar microstructure, and two having mixed equiaxed-columnar microstructures. In order to acquire reference field maps from a homogeneous-isotropic material, four carbon steel pipe sections that had an equivalent diameter and wall thickness were used. All samples were field pipe sections and had a 70-cm inner diameter and a 6-cm wall thickness, except the layered columnar-equiaxed microstructured block which had an 80-cm inner diameter and an 8-cm wall thickness.

Four spatial points were established on each block where an ultrasonic field map was to be acquired (Fig. 1). These points were used later as references for scanner alignment, microprobe placement, and aperture placement relative to the scanned material volume. The self-aligning fixture contained two guide holes separated by 5 cm along the length of the fixture. The two sets of paired spatial points enabled the pipe axial and circumferential axes to be defined as well as points which only differed in radial position and/or axial displacement.

Ultrasonic Field Map System

The ultrasonic field mapping system provided a two-dimensional map of the ultrasonic field (Fig. 2). Longitudinal-wave-field maps were obtained using a longitudinal-wave probe as a transmitter[a] and a longitudinal-wave microprobe as a receiver. A scan was accomplished by applying the microprobe[b] to a 45° facet and scanning in a raster format with the transmitting probe. RF data were stored and field maps determined by maximum absolute values in a 3.0 microsecond gate.

The post-gating process consisted of selecting six points dispersed throughout the scan aperture, centering the gate about the selected signal feature at each point, and checking the gate positions obtained by means of a second-ordered polynomial fit. The check was performed by observing multiple sequences of images displaying the RF signal with the superimposed gate (Fig. 3). The gating process resulted in mapping the quasi-steady-state response since the transmitter was excited by a five-cycle tone burst.

A technique improvement was placement of the longitudinal-wave microprobe on a 45° facet. Previous placement of the microprobe normal to the sample surface biased image features toward smaller refracted angles because of receiver directivity [2]. Directivity of the microprobe when applied to a 45° facet resulted in a ± 1 dB change in reception sensitivity over the angular range of 45° ± 20° for a facet machined into a plane and 45° ± 35° for a 45° facet machined into a right corner (Fig. 4). (Application of the microprobe to the corner was performed only for the sample having a layered microstructure due to the logistics of receiving a 45° refracted wave in a block having a thickness-to-axial-length ratio of 0.5.)

Ultrasonic field maps were formed by post-gating the digitized RF signals, determining the absolute peak response in the gated window, and determining dB values relative to the maximum gated amplitude value. The two-dimensional plot was made according to the coordinate system of the scanner and assigning color codes according to a

---

(a) The scrubbing surface of the acrylic wedge was contoured to match an outer pipe radius of 41 cm.
(b) The longitudinal-wave microprobe consisted of a 0.3-mm-diameter piezoelectric crystal at the end of a hollow metal needle.

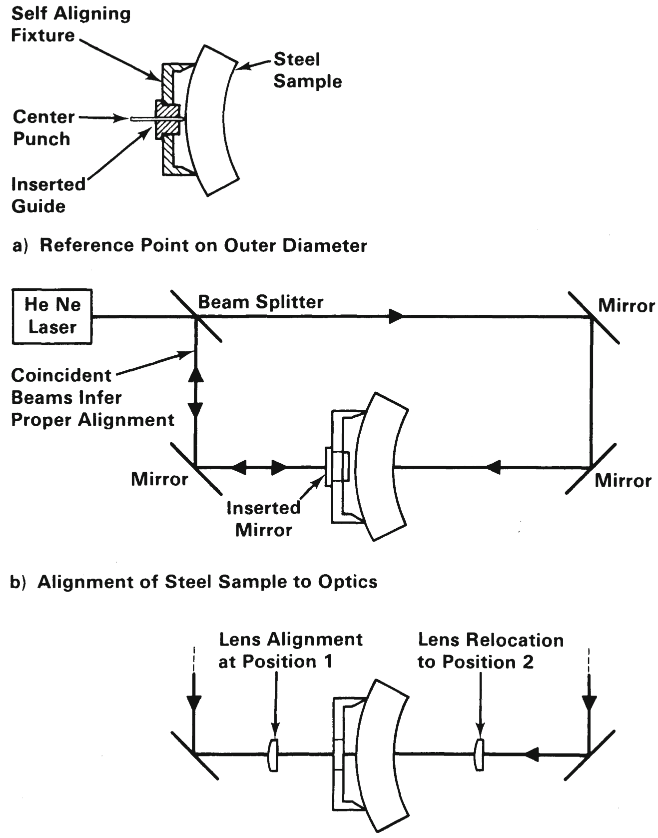

a) Reference Point on Outer Diameter

b) Alignment of Steel Sample to Optics

c) Reference Point on Inner Diameter

Fig. 1. Spatial points for referencing coordinates on steel samples

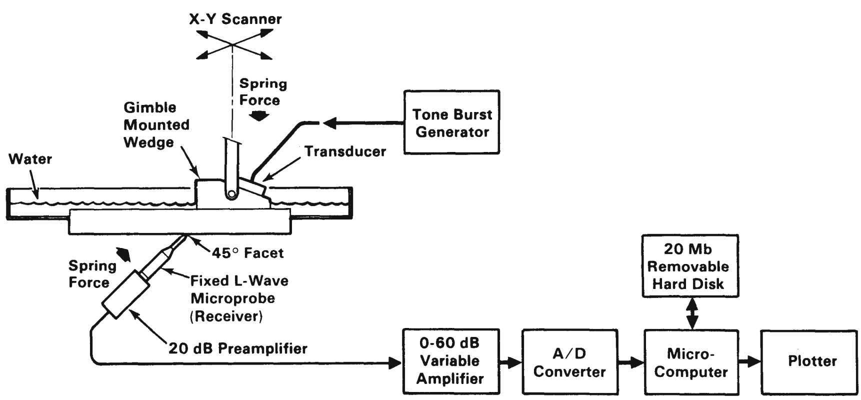

Fig. 2. Ultrasonic field mapping system for examining CCSS

preselected dB scale. Although one field map for each of the microstructural classifications was displayed (Fig. 5), four maps were taken, each in unique material volumes.

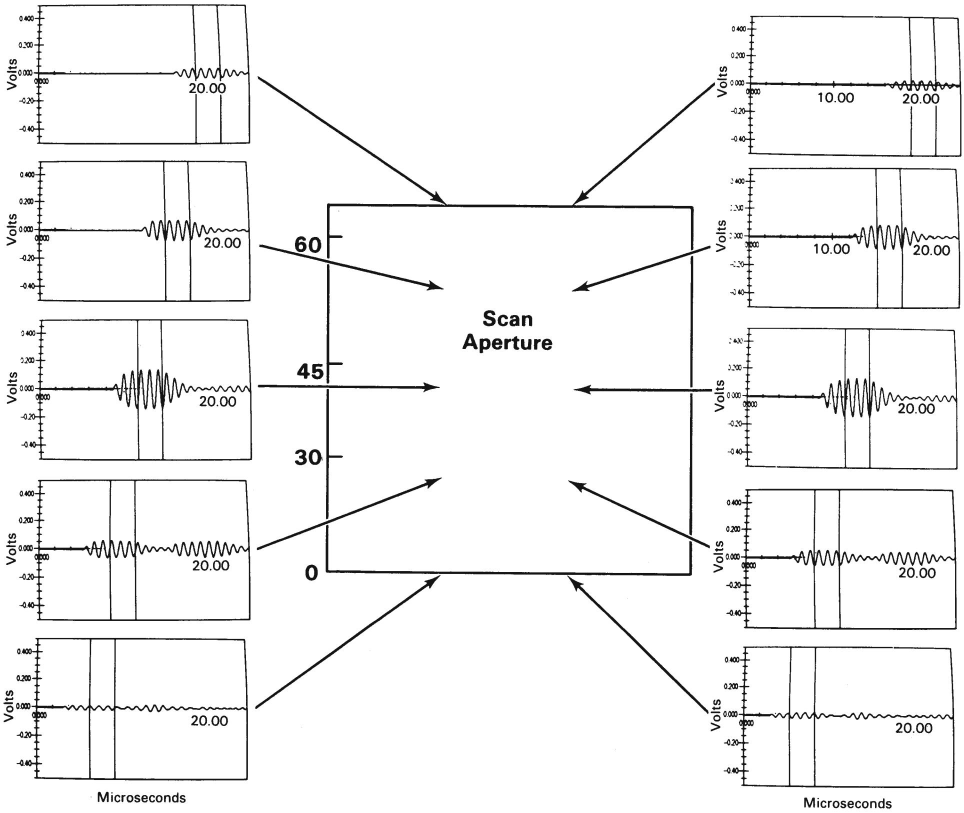

Fig. 3. Monitoring of gating process with windowed displays

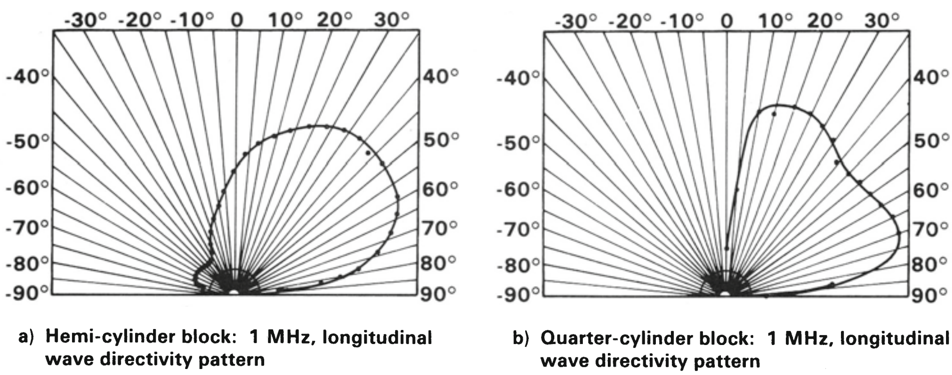

Fig. 4. Directivity of longitudinal-wave microprobe when applied to a 45° facet cut.

Data Analysis

The objectives of this work were to determine if a 1-MHz, 45°, longitudinal field maintained spatial coherence in all the microstructural forms of CCSS, to quantify the degree of distortion incurred by

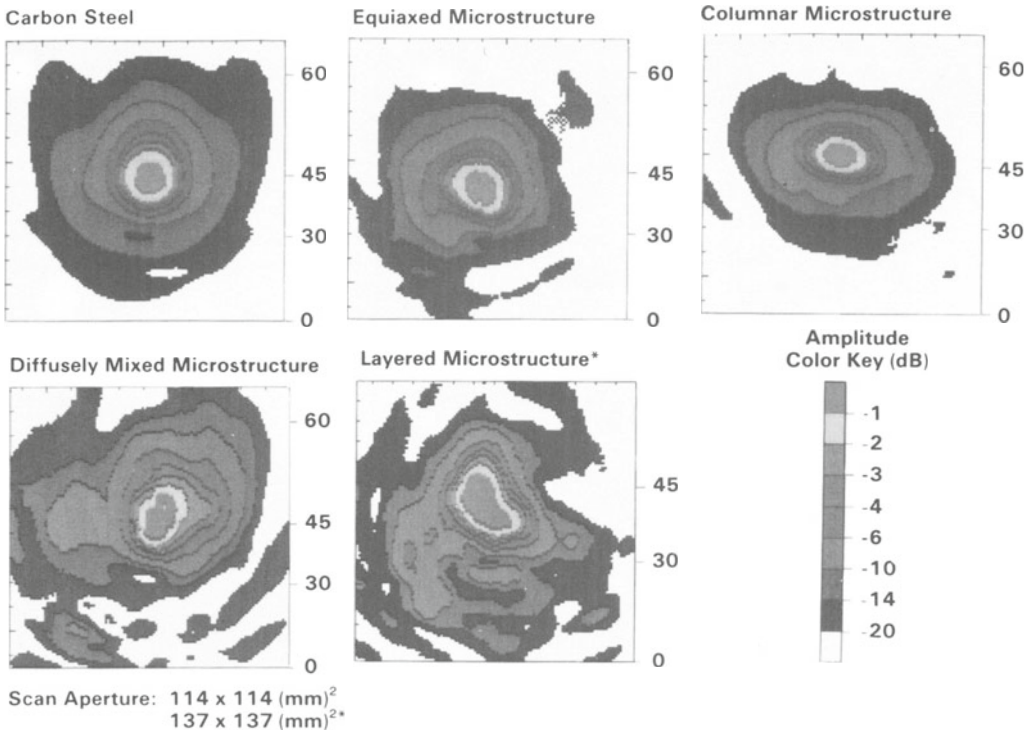

Fig. 5. Ultrasonic field maps of 1-MHz, 45°, longitudinal-wave fields

the ultrasonic field, and to evaluate if an effective ultrasonic inspection could be performed in all the CCSS microstructures. Spatial coherency was evaluated by examining all 20 field maps. Each field map except one (from the diffusely mixed microstructural sample) displayed an ultrasonic field in which the 0 to -3 dB region was contiguous. Thus, the spatial coherency of the transmitted field was rated as high for the pure microstructural forms of CCSS and as moderate for the mixed microstructural forms of CCSS.

Field distortion was evaluated by measuring the refracted angle and the positional variation of the field. Field position was defined as the center between the two extreme -1 dB transitions of the field map along either the circumferential or axial axis. The refracted angle was then calculated by a trigonometric relation between axial field position and pipe-wall thickness (Fig. 6).

The data from the equiaxed microstructure had a 43.6° mean which is close to that of the reference material (43.4°). The standard deviation of 1.0°, however, was three times higher than that of the reference material and indicative of the degree of inhomogeneity caused by large grains relative to a 1-MHz wave (6-mm wave length). (The 0.3° standard deviation from the reference material was believed to solely relate to set-up variations.)

The values from the columnar microstructure had a 46.1° mean which indicated that the maximum energy flow was redirected as predicted by anisotropic wave behavior. The standard deviation of 0.4° was effectively equal to that of the reference and indicated that the material appeared essentially as homogeneous as the reference material.

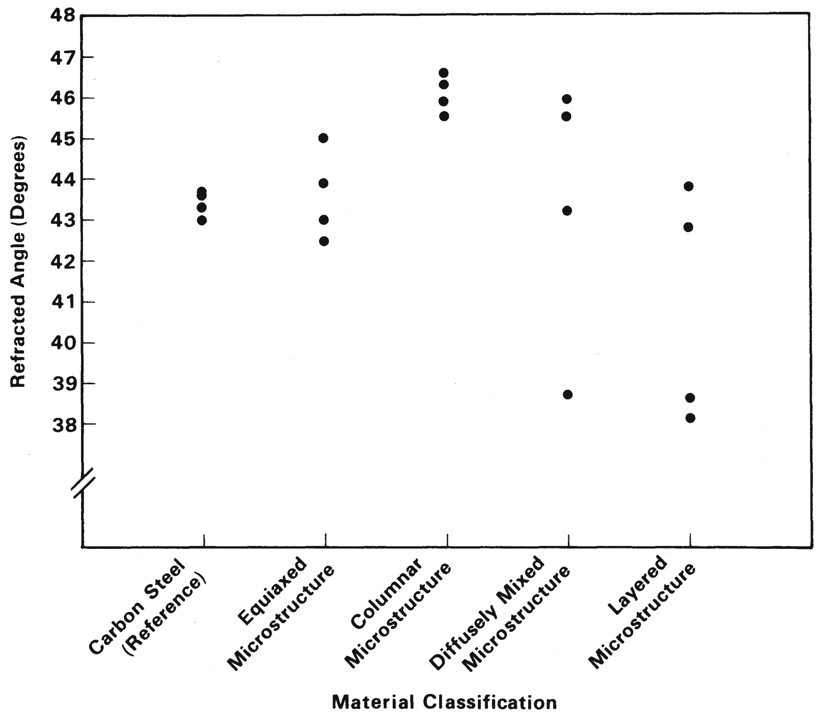

Fig. 6. Effective refracted angles of 1-MHz, 45°, longitudinal wave

Of the mixed-microstructures, data taken from the diffusely-mixed-microstructure had a 43.3° mean and a 2.9° standard deviation. This variation is 10 times higher than that of the reference material. The data from the layered-microstructure had a 40.8° mean and a 2.5° standard deviation which is 8 times higher than that of the reference material.

Significance of the refracted-angle results is the increased standard deviation of the equiaxed sample and the extremely large standard deviations of both materials having a mixed microstructure.

Another parameter selected to quantify field distortion was the field-position variation normalized to field width. When inspecting a selected material volume, sufficient field overlap is designed into the scan procedure to ensure detection sensitivity remains high for a defect anywhere within the material volume of interest. Obviously, if a small field width exists, then the allowable field displacement error must be small. Likewise, if a large field width exists, then the field-displacement error may be larger. Therefore, the field-position variation was normalized to field width and was calculated by measuring the difference between the extreme field positions unique to a microstructure and dividing by the smallest of the four -3 dB field widths. Values were obtained along both the circumferential and axial axes and are plotted in Fig. 7. As previously stated, the variations associated with the reference samples are assumed to be indicative of set-up variation and were 16% and 8% for the circumferential and axial values, respectively.

$$NFPV = \frac{RVFP}{MFW} \text{, where}$$

MFW is the Minimum of Measured 3 dB Field Widths and

RVFP is the Range of Variation in Field Position

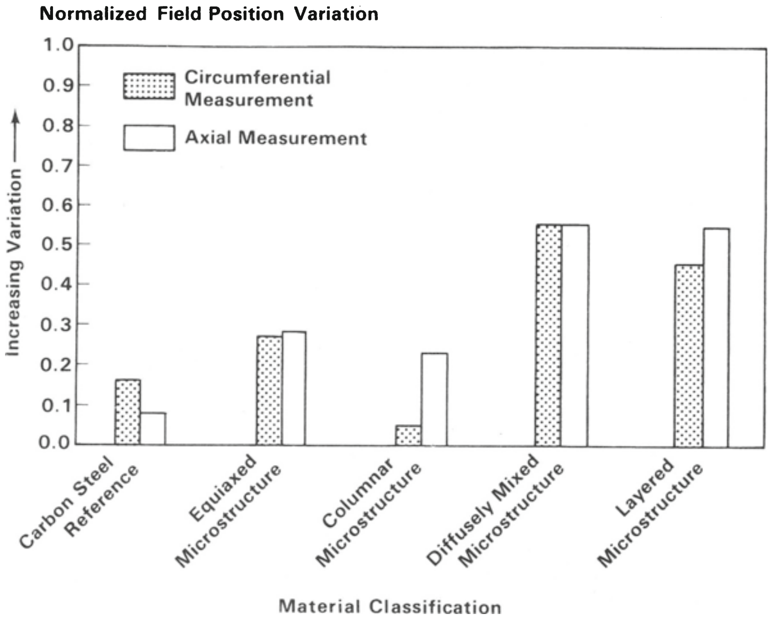

Fig. 7. Positional variation of longitudinal-wave fields

For CCSS material, increased variation was expected for the equiaxed material and ranged between 27% and 28% for values pertaining to measurement along both pipe axes. A low circumferential value of 5% was obtained for the columnar samples; however, the axial value was 23%. This latter value might initially seem high since the standard deviation of the refracted angle was small; however, the axial, -3 dB, field width of the columnar scans also is reduced and produces a higher normalized value. The two mixed microstructural forms had values ranging between 45% and 55%. This is alarming since scan patterns on a pipe may use circumferential increments as high as 50%. If two successive measurements are made and the field misdirection is outward from the two positions, then a material volume thought to be inspected by past procedures might be skipped.

CONCLUSIONS AND SUMMARY

Ultrasonic field maps were useful in evaluating the distortion resulting from a field propagating through a section of centrifugally cast stainless steel (CCSS) pipe. Through-transmission measurements employing a longitudinal-wave-microprobe receiver and a 1-MHz, 45°, longitudinal-wave transmitter with a 38-mm diameter crystal were used. Distortion was initially evaluated by examining 20 field maps to determine if the ultrasonic field maintained spatial coherency. Distortion was also examined by measuring parameters from the field maps and included the effective refracted angle and the variation of field-position normalized by field width. To quantify the distortional variation of a microstructure, four field maps were acquired from unique material volumes of each microstructural classification.

Spatial coherency of the transmitted ultrasonic field was rated high for the pure microstructural forms of CCSS and moderate for the mixed microstructural forms of CCSS. Further analysis indicated that the refracted angle varied between 38° and 47° for CCSS. The largest standard deviation of refracted angle occurred for the mixed microstructural forms (2.9°), which also had the largest normalized positional variation (0.55). These measurements indicate the increased difficulty of assuring a 50% field overlap when inspecting CCSS.

Due to the difference in field distortion, the worst-case material classification (mixed equiaxed-columnar microstructure) should be assumed for an inspection. An alternative is to continuously determine the microstructure as a scan is performed and to interrupt the data acquisition process and implement an appropriate technique customized to the detected microstructure when the probe passes to a different microstructure. This latter choice assumes an effective microstructural classifier and that an effective inspection technique exists for each of the possible microstructures.

Concerning field mapping in solids, the technique of applying a longitudinal-wave microprobe to a 45° facet for improved reception of a 45° longitudinal wave was benefical. Prior techniques of applying the microprobe normal to the far surface, biased image features toward smaller refracted angles because of receiver directivity. Application of the microprobe to the facet effected a ±1 dB change in recieving sensitivity over a broad angular range centered about 45°.

Future work is expected to continue analysis of the collected longitudinal-wave field maps and to perform both data acquisition and analysis of 500-kHz shear-wave fields (both vertically and horizontally polarized).

ACKNOWLEDGEMENTS

Work supported by the U.S. Nuclear Regulatory Commission under Contract DE-AC06-76RLO 1830; NRC Contract Monitor: Dr. J. Muscara; NRC FIN B2289.

The authors would like to express their gratitude to Mr. G. J. Posakony of PNL for his important contribution in the design and fabrication of the longitudinal-wave microprobe and to Southwest Research Institute and Westinghouse Electric Corporation for providing CCSS pipe sections.

REFERENCES

1. Good, M. S. and L. G. Van Fleet, in 8th International Conference on NDE in the Nuclear Industry, edited by D. Stahl (American Society for Metals International, Metals Park, Ohio, 1987) pp. 657-666.
2. Good, M. S. and L. G. Van Fleet, in Review of Progress in Quantitative Nondestructive Evaluation, edited by D. O. Thompson and D. E. Chimenti (Plenum Press, New York, 1988), Vol. 7A, pp. 637-646.